Specific heat in strongly hole-doped iron-based superconductors

Dmitry V. Chichinadze and Andrey V. Chubukov
School of Physics and Astronomy, University of Minnesota, Minneapolis, Minnesota 55455, USA

(Received 19 August 2018; revised manuscript received 8 November 2018; published 22 January 2019)

We compute specific heat $C(T)$ in a strongly hole-doped Fe-based superconductor, like KFe_2As_2, which has only hole pockets. We model the electronic structure by a three-orbital/three-pocket model with two smaller hole pockets made out of d_{xz} and d_{yz} orbitals and a larger pocket made out of d_{xy} orbital. We use as an input the experimental fact that the mass of d_{xy} fermion is several times heavier than that of d_{xz}/d_{yz} fermions. We argue that the heavy d_{xy} band gives the largest contribution to the specific heat in the normal state, but the superconducting gap on the d_{xy} pocket is much smaller than that on d_{xz}/d_{yz} pockets. We argue that in this situation the jump of $C(T)$ at T_c is determined by d_{xz}/d_{yz} fermions, and the ratio $(C_s - C_n)/C_n$ is a fraction of that in a one-band BCS superconductor. At $T < T_c$, $C(T)$ remains relatively flat down to some T^*, below which it rapidly drops. This behavior is consistent with the data for KFe_2As_2 and related materials. We use one-parameter model for the interactions and fix this only parameter by matching the experimental ratio of the gaps on the two d_{xz}/d_{yz} pockets. We argue that the resulting parameter-free model reproduces quantitatively the data on $C(T)$ for KFe_2As_2. We further argue that the very existence of a finite $T^* < T_c$ favors s^{+-} gap structure over d-wave, because in the latter case T^* would almost vanish.

DOI: 10.1103/PhysRevB.99.024509

I. INTRODUCTION

Rich physics of iron-based superconductors (FeSC) continues to attract strong attention from the condensed-matter community [1–13]. One of the most debated issues in the field is the strength of correlations. On one hand, FeSCs have Fermi surfaces, and most display a metallic, Fermi-liquid-like behavior in some temperature range above superconducting T_c. On the other, there is a clear distinction between the observed electronic structure and the one obtained by first-principle calculations for free fermions. Some researchers believe that this difference can be accounted for by including the momentum-dependent self-energy [14], which modifies the dispersion but leaves fermions and their collective degrees of freedom fully coherent (this is often termed as "itinerant scenario," see, e.g., Refs. [9,15]). Others argue that at energies relevant to superconductivity and competing orders, fermions can be viewed as correlated yet itinerant, but collective magnetic excitations should be viewed as at least partly localized (a "Hund metal scenario," see, e.g., Refs. [16,17]). And others further argue [18,19] that electronic excitations should be viewed as itinerant on some Fe orbitals and as nearly localized on other orbitals (an "orbital selective Mottness" scenario).

From the perspective of Mott physics, the best candidates to display Mott behavior are strongly hole-doped FeSCs, like KFe_2As_2 [20–25], as for these systems the tendency towards electron localization has been argued to develop at a smaller Hubbard U [18,19]. Low-energy fermionic states in KFe_2As_2 are composed of fermions from three orbitals, d_{xy}, d_{xz}, and d_{yz}, the last two are related by C_4 symmetry [20]. Specific heat measurements in KFe_2As_2 have shown that above superconducting T_c, specific heat coefficient $C(T)/T$ scales as $a + bT^2$, as expected in a metal, but a is larger than in other FeSCs [25–30]. Because a is proportional to the sum of the effective masses for different bands, a large value of a implies that at least one effective mass is large. Within the Mott scenario, the mass enhancement comes from frequency-dependent self-energy $\Sigma(\omega)$. This self-energy narrows the dispersion and simultaneously reduces the quasiparticle residue Z, transferring $1 - Z$ spectral weight into Hubbard subbands. The effect is believed to be the strongest for the band made of fermions from a d_{xy} orbital [18,19]. However, band narrowing and accompanying mass enhancement can be also caused by innocuous reasons like smaller hopping integral for d_{xy} fermions or closeness to a Van Hove singularity (see [31] and references therein). In the latter case, the large value of the specific heat coefficient can be understood already within the itinerant scenario. ARPES data do indeed show [31–33] that the d_{xy} band is more narrow than the bands made by fermions from d_{xz} and d_{yz} orbitals, but Hubbard subbands have not been yet detected in KFe_2As_2. Furthermore, some ARPES data on KFe_2As_2 and other FeSCs show that d_{xy} excitations are as sharp as excitations from d_{xz}/d_{yz} bands [21,34]. This makes the interpretation of specific heat data above T_c somewhat ambiguous.

In this article we analyze whether one can separate between Mott and itinerant scenarios by analyzing specific heat data in the superconducting state. Given that d_{xy} fermions have the largest mass, i.e., the largest density of states (DOS), there are four possibilities for system behavior below T_c. They are depicted in Fig. 1. One possibility [Fig. 1(a)] is that superconductivity predominantly develops on the heavy d_{xy} orbital because of larger DOS. If this is the case, the system's behavior is the same as in a one-band superconductor: the specific heat jump at T_c, $\delta C/C_n = (C_s - C_n)/C_n$, is of order one, and $C(T)$ varies as a function of a single variable T/T_c below T_c. Another [Fig. 1(b)] is that superconductivity develops at T_c on d_{xz}/d_{yz} orbitals, but the temperature dependence

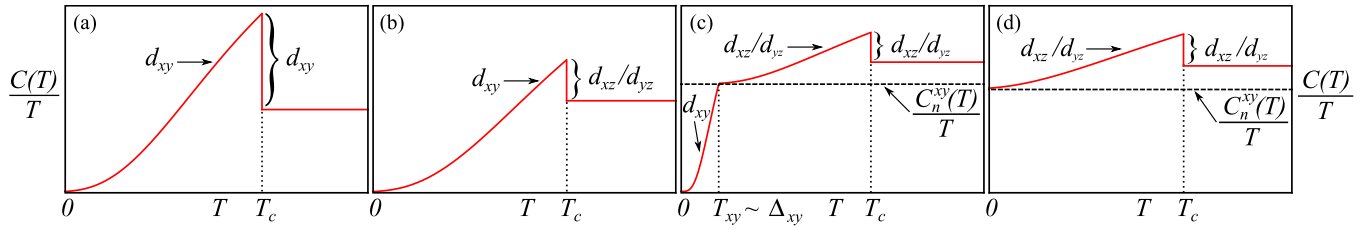

FIG. 1. Four different scenarios for the behavior of $C(T)/T$ in the three-pocket model with light d_{xz}/d_{yz} bands and a heavy d_{xy} band. (a) The specific heat both above and below T_c is determined by the d_{xy} band. (b) The specific heat jump is defined by the gap opening on d_{xz}/d_{yz} bands, but T dependence of $C(T)$ below T_c is still determined by the d_{xy} band. (c) The specific heat jump at T_c and the behavior at $T_{xy} < T < T_c$ is determined by d_{xz}/d_{yz} bands, while the contribution to $C(T)$ from the d_{xy} band remains the same as in the normal state (the dashed line). Below T_{xy}, the gap on the d_{xy} band becomes larger than T, and $C(T)/T$ rapidly drops. (d) The case when $T_{xy} = 0$.

of $C(T)$ below T_c is still determined by the heavy d_{xy} orbital. In this situation $\delta C/C_n$ is small, but $C(T)$ below T_c is the same as in Fig. 1(a). The third possibility [Fig. 1(c)] is that not only $(C_s - C_n)/C_n$ at T_c but also the behavior of $C(T)$ in some T range below T_c is determined by d_{xz}/d_{yz} orbitals, while fermions on the d_{xy} orbital have a smaller gap and can be treated as nonsuperconducting down to $T_{xy} < T_c$. In this situation $(C_s - C_n)/C_n$ is small, $C(T)/T$ varies slowly between T_c and T_{xy} towards a finite value [equal to normal state $C(T)/T$ for d_{xy} fermions], and rapidly drops below T_{xy}. And the fourth possibility [Fig. 1(d)] is that fermions on the d_{xy} orbital do not pair down to $T = 0$, i.e., $T_{xy} = 0$.

The data for KFe_2As_2 from several groups [25–30] show that (i) the specific heat jump at T_c is much smaller than the BCS value, (ii) between T_c and approximately $T_c/6$, $C(T)/T$ decreases rather slowly towards a finite value, and (iii) below $T_c/6$, $C(T)/T$ rapidly drops and tends to zero at $T \to 0$. This behavior is consistent with the one in Fig. 1(c). We analyze whether this behavior can be understood by just assuming that the d_{xy} band is heavier than the other two bands (and, hence, the DOS for this band is the largest), or one needs to additionally include the reduction of quasiparticle Z for the d_{xy} band. A momentum/frequency independent Z can be absorbed into the renormalization of the interactions involving d_{xy} fermions, hence the issue is whether mass/DOS variation between d_{xy} and d_{xz}/d_{yz} bands is sufficient to describe the data, or one needs to additionally assume that the interactions involving d_{xy} fermions are weaker than the ones between d_{xz} and d_{yz} fermions.

We argue that the difference in the masses is sufficient to describe the observed behavior. Namely, we obtain the behavior in Fig. 1(c) by analyzing the model of three Γ-centered d_{xz}/d_{yz} and d_{xy} hole pockets in the 2-Fe zone, and invoking mass difference but keeping the interactions on all three orbitals comparable in strength. If Z on the d_{xy} orbital is small in KFe_2As_2, this will additionally reduce the value of T_{xy}. We note in passing that our theoretical scenario is different from the one presented in Ref. [30] as we do not require that KFe_2As_2 is close to a magnetic quantum criticality. It is also different from the one in Ref. [26] where the temperature evolution of $C(T)$ was largely attributed to the gaps on hole barrels near (π, π) in the 2-Fe zone. We emphasize that the existing ARPES data did not detect superconducting gaps on the hole barrels, but did detect the gaps on the three Γ-centered hole pockets which we consider. Several earlier works [28,29] analyzed the behavior of $C(T)$ in KFe_2As_2 within the phenomenological two-gap model, constructed in analogy with the two-gap model for MgB_2 [35]. Our reasoning is similar to these works in the sense that we have larger gaps on d_{xz}/d_{yz} pockets and a smaller gap on D_{xy} pocket. On the other hand, our analysis is based microscopic three-band model, and we reproduce experimental $C(T)$ with no free parameters.

II. THE MODEL

The electronic structure of KFe_2As_2 in the physical 2-Fe Brillouin zone consists of three hole pockets, located at the Γ point, and hole barrels near (π, π). There is no evidence of superconductivity on the hole barrels, and we neglect them in our analysis. Two inner Γ-centered pockets are made out of fermions from d_{xz} and d_{yz} orbitals, and the outer pocket is made out of fermions from a d_{xy} orbital [20]. We take as an input that the d_{xy} band has larger band mass/DOS than d_{xz}/d_{yz} bands. We follow earlier works [36–39] and describe superconductivity within the low-energy model with $H = H_0 + H_{\rm int}$, where the quadratic Hamiltonian H_0 is given by a 2×2 matrix for d_{xz} and a separate term for d_{yz} fermions, and $H_{\rm int}$ is the Hubbard-Hund interaction, dressed by contributions from high-energy fermions.

To study superconductivity, we convert from orbital to band basis, i.e., diagonalize the quadratic form to $H_0 = \sum_k \varepsilon_{c,k} c_k^\dagger c_k + \varepsilon_{d,k} d_k^\dagger d_k + \varepsilon_{f,k} f_k^\dagger f_k$, where c_k and d_k are linear combinations of fermions from d_{xz} and d_{yz} orbitals, and f operators describe d_{xy} fermions. The pairing interaction has s-wave and d-wave components (see Ref. [37] and the Supplementary Material (SM) [40] for details). We focus first on s-wave superconductivity and discuss d-wave pairing later. The pairing interaction in an s-wave channel is

$$\begin{aligned} H_{\rm SC} &= \sum_{k,p,s\neq s'} [U_{cc} c_{sk}^\dagger c_{s'-k}^\dagger c_{s'p} c_{s-p} + U_{dd} d_{sk}^\dagger d_{s'-k}^\dagger d_{s'p} d_{s-p} \\ &+ U_{cd} (c_{sk}^\dagger c_{s'-k}^\dagger d_{s'p} d_{s-p} + \text{H.c.}) + U_{ff} f_{sk}^\dagger f_{s'-k}^\dagger f_{s'p} f_{s-p} \\ &+ (U_{fc} c_{sk}^\dagger c_{s'-k}^\dagger f_{s'p} f_{s-p} + U_{fd} d_{sk}^\dagger d_{s'-k}^\dagger f_{s'p} f_{s-p} + \text{H.c.})], \end{aligned} \tag{1}$$

where for circular hole pockets, bare interactions are $U_{cc} = U_{dd} = U_{cd} = (U + J')/2$, $U_{ff} = U/2$, and $U_{fc} = U_{fd} = \frac{J'}{2}$. After renormalizations from high-energy fermions,

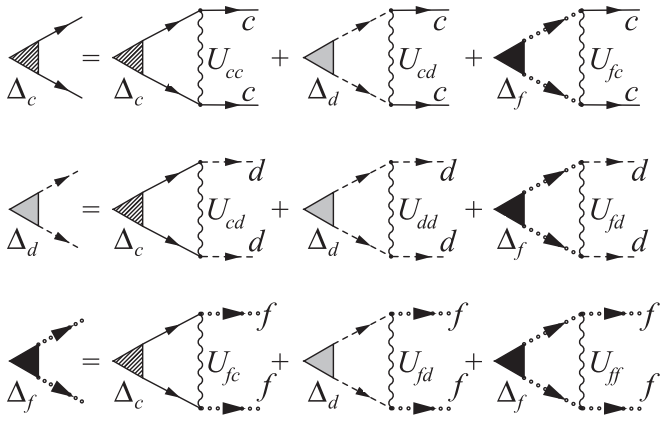

FIG. 2. Diagrammatic expressions for Gorkov's gap equations. Triangles with different filling represent SC vertexes on different bands. Solid, dashed, and dotted lines represent c, d, and f fermions, respectively. Wavy lines represent interactions between fermions.

all couplings become different, and, most important, U_{cd}^2 becomes larger than $U_{cc}U_{dd}$ [37,38,41]. This gives rise to an attraction in the s^{+-} channel.

III. SUPERCONDUCTIVITY

Superconducting T_c and s-wave gaps on the three Γ-centered hole pockets at $T \leqslant T_c$ are obtained by solving the set of coupled linearized gap equations, presented in Fig. 2. In analytical form we have

$$\begin{pmatrix}\Delta_c\\ \Delta_d\\ \Delta_f\end{pmatrix} = -L\begin{pmatrix}\nu_c U_{cc} & \nu_d U_{cd} & \nu_f U_{fc}\\ \nu_c U_{cd} & \nu_d U_{dd} & \nu_f U_{fd}\\ \nu_c U_{fc} & \nu_d U_{fd} & \nu_f U_{ff}\end{pmatrix}\begin{pmatrix}\Delta_c\\ \Delta_d\\ \Delta_f\end{pmatrix}, \quad (2)$$

where $L = \ln\frac{\Lambda}{T_c}$, Λ is the upper cutoff, and ν_c, ν_d,, and ν_f are densities of states, proportional to the band masses. In our case, $\nu_c \sim \nu_d$, and ν_f is larger. We present the full solution for the gap in the SM and here show the result for $\vec{\Delta} = (\Delta_c, \Delta_d, \Delta_f)^T = (1, \alpha, -\beta\frac{\nu_c}{\nu_f})^T$ to leading order in $\nu_{c,d}/\nu_f$, where α and β do not depend on ν_f (see SM for exact expressions). The key observation here is that the gap Δ_f on the d_{xy} pocket is small in the ratio of $\nu_{c,d}/\nu_f$. This is the consequence of the fact that s^{+-} superconductivity develops on c and d pockets (not to be confused with s^{+-} pairing in systems with both electron and hole pockets), while the gap on the d_{xy} pocket does not develop on its own, but rather is induced by interorbital pairing interactions (Δ_f scales with U_{fc}, U_{fd}). Note that Δ_f is nonzero only when c and d pockets are treated as nonequivalent, otherwise $\alpha = -1$ and $\beta = 0$.

To minimize the number of parameters, below we set U_{cd}, U_{ff}, U_{fc}, and U_{fd} equal to their bare values in the Hubbard-Hund model (see above) and use $J = J' = 0.4U$ [39]. Then $U_{cd} = 0.7U$, $U_{ff} = 0.5U$, and $U_{fc} = U_{fd} = 0.2U$ [10,42]. We model the renormalization of $U_{cd}^2 - U_{cc}U_{dd}$ into a positive variable, necessary for s^{+-} superconductivity, by a single parameter x, by setting $U_{cc} = U_{cc}^{\text{bare}}(1-x) = 0.7U(1-x)$ and $U_{dd} = U_{dd}^{\text{bare}}(1+x) = 0.7U(1+x)$. We used the experimental values $\nu_d/\nu_c = 1.33$ and $\nu_f/\nu_c = 3.17$ from Ref. [30] and set $x = 0.5$ to match the experimental value of $\alpha \approx -0.4$ [20]. The same x gives $\beta\nu_c/\nu_f \sim 0.06$, consistent with [20].

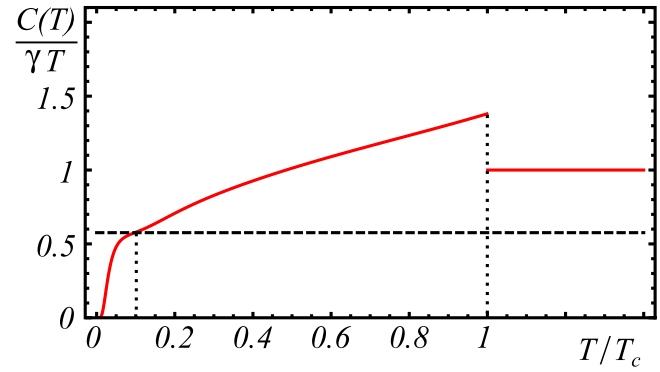

FIG. 3. The result of the numerical evaluation of the specific heat coefficient $C(T)/(\gamma T)$ within our model [$C(T) = \gamma T$ above T_c]. The dashed line shows $C(T)/(\gamma T)$ for d_{xy} orbital in the normal state. The magnitude of the jump of $C(T)$ at T_c and the overall behavior of $C(T)/(\gamma T)$ below T_c agrees well with the experimental data from [25,28–30,43–45].

IV. THE SPECIFIC HEAT

To calculate $C(T)$, we compute the internal energy $E(T)$ above and below T_c and use $C(T) = dE/dT$. To obtain $E(T)$ we construct a BCS Hamiltonian with anomalous terms with prefactors Δ_c, Δ_d, and Δ_f, and diagonalize it. This yields

$$E(T) = -\sum_{i=c,d,f}\nu_i\int d\varepsilon_i\frac{\varepsilon_i^2+\Delta_i^2/2}{\sqrt{\varepsilon_i^2+\Delta_i^2}}\tanh\frac{\sqrt{\varepsilon_i^2+\Delta_i^2}}{2T} + \cdots, \quad (3)$$

where dots stand for temperature-independent terms. We express Δ_d and Δ_f via Δ_c and $E(T)$ in powers of Δ_c. To first order in $\nu_{c,d}/\nu_f$ we obtain $E(T) = E(T_c) - (\nu_c + \nu_d\alpha^2)|\Delta_c|^2/2$. The contribution from the f band is small in $\nu_{c,d}/\nu_f$ despite that the DOS for this band is large. Using $\Delta_c(T) \propto \sqrt{T_c - T}$, we then obtain that the magnitude of the jump of the specific heat at T_c does not depend on ν_f. The specific heat above T_c, on the other hand, comes primarily from the d_{xy} band simply because DOS for this band is the largest. As a result, $\delta C/C_n \propto \nu_{c,d}/\nu_f$ is small, unlike in a one-band BCS superconductor, where it is $O(1)$. We present the full expression for $\delta C/C_n$ in the SM.

To obtain $C(T)$ below T_c, we assume, following [12] that the ratios Δ_d/Δ_c and Δ_f/Δ_c remain the same as near T_c, and $\Delta_c(T)$ has the same temperature dependence as in BCS superconductor. We then find from (3) that in the T range where $\Delta_f(T) \approx -(\beta\nu_c/\nu_f)\Delta_c(T)$ is smaller than T, the contribution to the specific heat from the d_{xy} band remains the same as in the normal state. As the consequence, $C(T)/T$ evolves from its maximal value right below T_c to a finite value equal to the specific heat coefficient from nonsuperconducting d_{xy} band. This behavior changes below $T \sim T_{xy}$, at which $\Delta_f(T_{xy}) = T_{xy}$. At such low temperatures the gap on the d_{xy} band cannot be neglected, and the contribution to the specific heat from this band rapidly drops, and, as a result, $C(T)/T$ rapidly drops towards zero value at $T = 0$.

In Fig. 3 we show the result of numerical calculation of the specific heat coefficient, using experimental values

from the DOSs from Ref. [30]. The behavior is the same as presented schematically in Fig. 1(c), and agrees *quantitatively* with the experimental data for KFe_2As_2 [25,28–30,43–45]. We emphasize that we fixed the only interaction parameter x by matching the measured [20] ratio of Δ_d/Δ_c, hence our $C(T)$ is obtained with no fitting parameters. We reproduce the experimental location of T_{xy}, and the overall behavior of $C(T)$ below T_c.

V. *d*-WAVE PAIRING

Some experimental data, most notably on the thermal conductivity [46,47], have been interpreted as evidence for d-wave pairing symmetry in KFe_2As_2. This is in variance with laser ARPES study [20,24], whose results were interpreted as evidence for the s-wave pairing. Theoretical results show that s-wave and d-wave pairing components are both attractive and comparable in strength, with RPA calculations [38] favoring s^{+-} superconductivity and early functional RG calculations [48] favoring d-wave pairing. By all these reasons, it is instructive to analyze $C(T)$ for d-wave pairing.

Within our model of circular pockets, d-wave pairing involves only c and d pockets. The d-wave component of the pairing interaction is

$$H_{\rm SC} = \sum_{k,p,s\neq s'} [\tilde{U}_{cc} c^\dagger_{sk} c^\dagger_{s'-k} c_{s'p} c_{s-p} + \tilde{U}_{dd} d^\dagger_{sk} d^\dagger_{s'-k} d_{s'p} d_{s-p} - \tilde{U}_{cd} (c^\dagger_{sk} c^\dagger_{s'-k} d_{s'p} d_{s-p} + \text{H.c.})] \cos 2\phi_k \cos 2\phi_p, \quad (4)$$

where ϕ_k and ϕ_p are angles along the Fermi surfaces. At the bare level (i.e., without integrating out high-energy fermions) $\tilde{U}_{cc} = \tilde{U}_{dd} = \tilde{U}_{cd} = (U - J')/2$. There also exists the $\sin 2\phi_k \sin 2\phi_p$ interaction component, but it does not give rise to new physics and we skip it. After renormalization $\tilde{U}_{cc}$ and $\tilde{U}_{dd}$ split, and, most importantly, $\tilde{U}^2_{cd}$ becomes larger than $\tilde{U}_{cc}\tilde{U}_{dd}$ [49]. Like for the s^{+-} case, the enhancement of the interpocket pairing interaction gives rise to an attraction and a nonzero T_c for d-wave pairing. The matrix equation for the d-wave gap is

$$\begin{pmatrix} \Delta_c \\ \Delta_d \end{pmatrix} = -\frac{L}{2} \begin{pmatrix} \nu_c \tilde{U}_{cc} & -\nu_d \tilde{U}_{cd} \\ -\nu_c \tilde{U}_{cd} & \nu_d \tilde{U}_{dd} \end{pmatrix} \begin{pmatrix} \Delta_c \\ \Delta_d \end{pmatrix}. \quad (5)$$

Evaluating the eigenfunctions, substituting them into the expression for the internal energy $E(T)$, and differentiating over T, we obtain the behavior as in Fig. 1(d). Namely, the jump $\delta C/C_n$ at T_c is small, and $C(T)/T$ below T_c drops but tends to a finite value at $T = 0$, equal to $C(T)/T$ for nonsuperconducting d_{xy} band. This does not agree with the data, which clearly show that $C(T)/T$ drops below $T_{xy} < T_c$. This result holds for arbitrary C_4-symmetric dispersion, as long as the interaction in the orbital basis is local, and the larger hole pocket can be approximated as pure d_{xy}. By all accounts (see, e.g., Ref. [12]), the admixture of d_{xz}/d_{yz} orbital states to the composition of this pocket is very small (a percent), so T_{xy}, even if finite, should be truly small.

VI. CONCLUSIONS

In this paper we studied the specific heat of KFe_2As_2. We argued that $C(T)$ in the normal state is chiefly determined by the heavy d_{xy} pocket, however superconductivity predominantly involves d_{xz}/d_{yz} pockets, while the gap on the d_{xy} pocket is either induced, but is small (for s-wave pairing), or not induced at all (for d-wave pairing). This gives rise to the behavior when (i) the jump of $C(T)$ at T_c is much smaller than the BCS value, and (ii) below T_c specific heat coefficient $C(T)/T$ initially evolves towards a finite value, equal to normal state contribution from d_{xy} band. For s-wave pairing, $C(T)/T$ eventually drops below a certain T_{xy} [Figs. 1(c) and 3]. If the pairing is d-wave, $T_{xy} = 0$ in our analysis, and is likely quite small in a more general case. The experimentally detected behavior of $C(T)/T$ [25,28–30,43,44] is more consistent with s-wave pairing. We used the detuning of interactions on d_{xz} and d_{yz} pockets from their bare values as a single adjustable parameter to reproduce the data on gap ratio on the two small pockets [20]. After that, our theory has no free parameters. It reproduces the magnitude of the jump at T_c, the shape of $C(T)/T$ below T_c, and the value of T_{xy}. We emphasize that we did not assume that interactions involving d_{xy} fermions are additionally reduced due to potentially small quasiparticle residue Z for fermions on the d_{xy} band. The reduction of Z_{xy} under hole doping follows from quite solid theoretical arguments [17,18], what is less clear is whether the reduction is strong enough to affect $C(T)$. If it is, the overall behavior of $C(T)/T$ will not change compared to our analysis, but T_{xy} will decrease further compared to T_c. A systematic study of $C(T)$ in doped $K_{1-x}Ba_xFe_2As_2$ is needed to determine the influence of Z_{xy} on the specific heat.

ACKNOWLEDGMENTS

We thank R. Fernandes, F. Hardy, H. v Löhneysen, D. Shaffer, and R.-Q. Xing for useful discussions. The work was supported by the Office of Basic Energy Sciences, U.S. Department of Energy, under Award No. DE-SC0014402 (A.V.C.).

[1] K. Ishida, Y. Nakai, and H. Hosono, J. Phys. Soc. Jpn. **78**, 062001 (2009).
[2] D. C. Johnston, Adv. Phys. **59**, 803 (2010).
[3] I. I. Mazin, Nature (London) **464**, 183 (2010).
[4] J. Paglione and R. L. Greene, Nat. Phys. **6**, 645 (2010).
[5] H.-H. Wen and S. Li, Annu. Rev. Condens. Matter Phys. **2**, 121 (2011).
[6] D. Basov and A. V. Chubukov, Nat. Phys. **7**, 272 (2011).
[7] P. J. Hirschfeld, M. M. Korshunov, and I. I. Mazin, Rep. Prog. Phys. **74**, 124508 (2011).
[8] G. R. Stewart, Rev. Mod. Phys. **83**, 1589 (2011).
[9] A. Chubukov, Annu. Rev. Condens. Matter Phys. **3**, 57 (2012).
[10] E. Bascones, B. Valenzuela, and M. J. Calderón, C. R. Phys. **17**, 36 (2016).
[11] A. V. Chubukov and P. J. Hirschfeld, Phys. Today **68**, 46 (2015).

[12] S. Graser, T. A. Maier, P. J. Hirschfeld, and D. J. Scalapino, New J. Phys. **11**, 025016 (2009).

[13] R. Fernandes, A. Chubukov, and J. Schmalian, Nat. Phys. **10**, 97 (2014).

[14] L. Ortenzi, E. Cappelluti, L. Benfatto, and L. Pietronero, Phys. Rev. Lett. **103**, 046404 (2009).

[15] A. Chubukov, Itinerant electron scenario, in *Iron-Based Superconductivity*, edited by D. P. Johnson, G. Xu, and W.-G. Yin (Springer International, Cham, 2015), pp. 255–329.

[16] Z. Yin, K. Haule, and G. Kotliar, Nat. Mater. **10**, 932 (2011).

[17] L. de' Medici, Hund's metals, explained, in *The Physics of Correlated Insulators, Metals, and Superconductors*, edited by E. Pavarini, E. Koch, R. Scalettar, and R. Martin (Verlag des Forschungszentrum Julich, 2017).

[18] L. de' Medici, G. Giovannetti, and M. Capone, Phys. Rev. Lett. **112**, 177001 (2014).

[19] L. de' Medici, Weak and strong correlations in Fe superconductors, in *Iron-Based Superconductivity*, edited by D. P. Johnson, G. Xu, and W.-G. Yin (Springer International, Cham, 2015), pp. 409–441.

[20] K. Okazaki, Y. Ota, Y. Kotani, W. Malaeb, Y. Ishida, T. Shimojima, T. Kiss, S. Watanabe, C.-T. Chen, K. Kihou, C. H. Lee, A. Iyo, H. Eisaki, T. Saito, H. Fukazawa, Y. Kohori, K. Hashimoto, T. Shibauchi, Y. Matsuda, H. Ikeda, H. Miyahara, R. Arita, A. Chainani, and S. Shin, Science **337**, 1314 (2012).

[21] T. Sato, K. Nakayama, Y. Sekiba, P. Richard, Y.-M. Xu, S. Souma, T. Takahashi, G. F. Chen, J. L. Luo, N. L. Wang, and H. Ding, Phys. Rev. Lett. **103**, 047002 (2009).

[22] V. Zabolotnyy, D. Evtushinsky, A. Kordyuk, D. Inosov, A. Koitzsch, A. Boris, G. Sun, C. Lin, M. Knupfer, B. Büchner, A. Varykhalov, R. Follath, and S. Borisenko, Physica C **469**, 448 (2009).

[23] T. Terashima, M. Kimata, N. Kurita, H. Satsukawa, A. Harada, K. Hazama, M. Imai, A. Sato, K. Kihou, C.-H. Lee, H. Kito, H. Eisaki, A. Iyo, T. Saito, H. Fukazawa, Y. Kohori, H. Harima, and S. Uji, J. Phys. Soc. Jpn. **79**, 053702 (2010).

[24] Y. Ota, K. Okazaki, Y. Kotani, T. Shimojima, W. Malaeb, S. Watanabe, C.-T. Chen, K. Kihou, C. H. Lee, A. Iyo, H. Eisaki, T. Saito, H. Fukazawa, Y. Kohori, and S. Shin, Phys. Rev. B **89**, 081103 (2014).

[25] F. Hardy, R. Eder, M. Jackson, D. Aoki, C. Paulsen, T. Wolf, P. Burger, A. Böhmer, P. Schweiss, P. Adelmann, R. A. Fisher, and C. Meingast, J. Phys. Soc. Jpn. **83**, 014711 (2014).

[26] F. Hardy, A. E. Böhmer, D. Aoki, P. Burger, T. Wolf, P. Schweiss, R. Heid, P. Adelmann, Y. X. Yao, G. Kotliar, J. Schmalian, and C. Meingast, Phys. Rev. Lett. **111**, 027002 (2013).

[27] S. L. Bud'ko, Y. Liu, T. A. Lograsso, and P. C. Canfield, Phys. Rev. B **86**, 224514 (2012).

[28] M. Abdel-Hafiez, S. Aswartham, S. Wurmehl, V. Grinenko, C. Hess, S.-L. Drechsler, S. Johnston, A. U. B. Wolter, B. Büchner, H. Rosner, and L. Boeri, Phys. Rev. B **85**, 134533 (2012).

[29] H. Fukazawa, Y. Yamada, K. Kondo, T. Saito, Y. Kohori, K. Kuga, Y. Matsumoto, S. Nakatsuji, H. Kito, P. M. Shirage, K. Kihou, N. Takeshita, C.-H. Lee, A. Iyo, and H. Eisaki, J. Phys. Soc. Jpn. **78**, 083712 (2009).

[30] F. Eilers, K. Grube, D. A. Zocco, T. Wolf, M. Merz, P. Schweiss, R. Heid, R. Eder, R. Yu, J.-X. Zhu, Q. Si, T. Shibauchi, and H. v. Löhneysen, Phys. Rev. Lett. **116**, 237003 (2016).

[31] S.-L. Drechsler, H. Rosner, V. Grinenko, S. Aswartham, I. Morozov, M. Liu, A. Boltalin, K. Kihou, C. H. Lee, T. Kim, D. Evtushinsky, J. M. Tomczak, S. Johnston, and S. Borisenko, J. Supercond. Novel Magn. **31**, 777 (2018).

[32] L. C. Rhodes, M. D. Watson, A. A. Haghighirad, D. V. Evtushinsky, M. Eschrig, and T. K. Kim, Phys. Rev. B **98**, 180503(R) (2018).

[33] D. V. Evtushinsky, V. B. Zabolotnyy, L. Harnagea, A. N. Yaresko, S. Thirupathaiah, A. A. Kordyuk, J. Maletz, S. Aswartham, S. Wurmehl, E. Rienks, R. Follath, B. Büchner, and S. V. Borisenko, Phys. Rev. B **87**, 094501 (2013).

[34] Z. R. Ye, Y. Zhang, F. Chen, M. Xu, J. Jiang, X. H. Niu, C. H. P. Wen, L. Y. Xing, X. C. Wang, C. Q. Jin, B. P. Xie, and D. L. Feng, Phys. Rev. X **4**, 031041 (2014).

[35] A. A. Golubov, J. Kortus, O. V. Dolgov, O. Jepsen, Y. Kong, O. K. Andersen, B. J. Gibson, K. Ahn, and R. K. Kremer, J. Phys.: Condens. Matter **14**, 1353 (2002).

[36] V. Cvetkovic and O. Vafek, Phys. Rev. B **88**, 134510 (2013).

[37] O. Vafek and A. V. Chubukov, Phys. Rev. Lett. **118**, 087003 (2017).

[38] S. Maiti, M. M. Korshunov, and A. V. Chubukov, Phys. Rev. B **85**, 014511 (2012).

[39] L. Classen, R.-Q. Xing, M. Khodas, and A. V. Chubukov, Phys. Rev. Lett. **118**, 037001 (2017).

[40] See Supplemental Material at http://link.aps.org/supplemental/10.1103/PhysRevB.99.024509 for the details of the computations.

[41] A. V. Chubukov, M. Khodas, and R. M. Fernandes, Phys. Rev. X **6**, 041045 (2016).

[42] A. Georges, L. d. Medici, and J. Mravlje, Annu. Rev. Condens. Matter Phys. **4**, 137 (2013).

[43] J. G. Storey, J. W. Loram, J. R. Cooper, Z. Bukowski, and J. Karpinski, Phys. Rev. B **88**, 144502 (2013).

[44] J. S. Kim, E. G. Kim, G. R. Stewart, X. H. Chen, and X. F. Wang, Phys. Rev. B **83**, 172502 (2011).

[45] V. Grinenko, D. V. Efremov, S.-L. Drechsler, S. Aswartham, D. Gruner, M. Roslova, I. Morozov, K. Nenkov, S. Wurmehl, A. U. B. Wolter, B. Holzapfel, and B. Büchner, Phys. Rev. B **89**, 060504 (2014).

[46] F. Tafti, A. Juneau-Fecteau, M.-E. Delage, S. R. De Cotret, J.-P. Reid, A. Wang, X. Luo, X. Chen, N. Doiron-Leyraud, and L. Taillefer, Nat. Phys. **9**, 349 (2013).

[47] M. Abdel-Hafiez, V. Grinenko, S. Aswartham, I. Morozov, M. Roslova, O. Vakaliuk, S. Johnston, D. V. Efremov, J. van den Brink, H. Rosner, M. Kumar, C. Hess, S. Wurmehl, A. U. B. Wolter, B. Büchner, E. L. Green, J. Wosnitza, P. Vogt, A. Reifenberger, C. Enss, M. Hempel, R. Klingeler, and S.-L. Drechsler, Phys. Rev. B **87**, 180507 (2013).

[48] R. Thomale, C. Platt, W. Hanke, J. Hu, and B. A. Bernevig, Phys. Rev. Lett. **107**, 117001 (2011).

[49] R.-Q. Xing, L. Classen, and A. V. Chubukov, Phys. Rev. B **98**, 041108 (2018).